CHEMISTRY
A EUROPEAN JOURNAL

DOI: 10.1002/chem.200700408

Bond Paths as Privileged Exchange Channels

A. Martín Pendás,*[a] Evelio Francisco,[a] Miguel A. Blanco,[a] and Carlo Gatti[b]

Abstract: Evidence that the bond paths of the quantum theory of atoms-in-molecules (QTAIM) signal preferred quantum-mechanical exchange channels is presented. We show how bond paths between an atom A and the atoms B in its environment appear to be determined by competition among the A–B exchange-correlation energies that always contribute to stabilize the A–B interactions. These pairwise additive stabilizations depend neither on the attractive or repulsive nature of the classical electrostatic interaction between the atoms' charge densities, nor on the change in the self energies of the atoms involved. These other terms may well cause an overall molecular-energy increase in spite of a possibly large A–B exchange-correlation stabilization. After our proposal, bond paths, both at and out of equilibrium geometries, are endowed with a specific energetic meaning that should contribute to reconcile the orthodox QTAIM interpretation with other widely accepted views, and to settle recent controversies questioning the meaning of hydrogen–hydrogen bonding and the nature of the so-called "steric interactions", the role of bond paths in endohedral complexes, and the generality of the results provided by the QTAIM. Implications for the nature of more general closed-shell interactions are also briefly discussed.

Keywords: bond energy · bond theory · electronic structure · energy decompositions · quantum theory of atoms-in-molecules (QTAIM)

Introduction

Real-space analyses of wavefunctions have contributed much to enrich the theory of chemical bonding, supplementing the dominant molecular orbital (MO) view with orbital invariant quantities whose definition and interpretation does not depend on the particular route taken to obtain the wavefunction (e.g., its one- or multideterminant character, its valence-bond or MO origin). Among these, the quantum theory of atoms-in-molecules (QTAIM) of Bader and coworkers[1] stands as one of the best-known, most-cited real-space approaches, this being a consequence of its elegance, mathematical simplicity, and deep physicochemical insight it has provided over the years.

The outstanding position of the QTAIM has been accompanied, as part of the conventional falsification-based scientific procedure, by intense periodic waves of scrutiny, affecting both its foundations,[2–4] and the relation between its central quantities and similar (although not necessarily identical) concepts in other approaches to chemical bonding. One of the recurrent criticisms that we encounter is related to the physical meaning of bond paths (BPs) or bond critical points (BCPs) in the electron-density scalar field $\rho(\boldsymbol{r})$. According to the, let us say, *orthodox* QTAIM interpretation,[1] the presence of a BP between two atoms is a necessary and sufficient condition for the atoms to be bonded to one another when there are no net forces acting on the nuclei.

However impressive the ability of such a simple recipe to algorithmically recover the chemists' lines drawn between atoms, it has become clear that not all BPs are found where chemists will find *bonds*.[5] Bader has repeatedly noted that the approximate homeomorphism between the virial and the electron-density fields[6,7] assures that the presence of a BP at or near equilibrium molecular geometries (so a mirror virial path exists in the virial field) warrants an energy lowering, thus confirming the formation of a bond. In recent years,[8] the existence of attractive Ehrenfest forces across the surface separating bonded atoms has reinforced such statements.

One well-known example of disagreement between the QTAIM and classical views is the presence of BPs between sterically crowded atoms, as shown by Cioslowski and Mixon[9] in *ortho*-substituted biphenyls. These authors pro-

---

[a] Prof. A. M. Pendás, Prof. E. Francisco, Prof. M. A. Blanco
Departamento de Química Física y Analítica
Facultad de Química, Universidad de Oviedo
33006 Oviedo (Spain)
Fax: (+34) 985-103-125
E-mail: angel@fluor.quimica.uniovi.es

[b] Dr. C. Gatti
CNR-ISTM Istituto di Scienze e Tecnologie Molecolari
Via Golgi 19, 20133 Milano (Italy)

© 2007 Wiley-VCH Verlag GmbH & Co. KGaA, Weinheim

posed that BPs signaled either bonding (attractive) or nonbonding (steric, repulsive) interactions. Other interesting cases include the ubiquitous anion–anion BPs found in many inorganic solids,[10] which have also been interpreted by some authors as clear cases of nonbonding interactions. A recent work by Haaland, Shorokhov, and Tverdova[11] showing the existence, and criticizing the meaning of He−C BPs in the metastable He@adamantane endohedral complex, was thoroughly contested by Bader and Fang.[8] This, together with a paper by Matta et al.[12] claiming the existence of generalized H−H bonding situations, including those between the two *ortho* hydrogens in the planar transition state of biphenyl, has triggered a new wave of intense debates. For instance,[13,14] Poater, Solà, and Bickelhaupt used the Ziegler–Rauk[15,16] energy decomposition analysis (EDA) to purportedly falsify the existence of H−H bonding, reporting that the classical steric repulsion is in fact responsible for the twisted geometry of biphenyl, and that many of the central concepts of the QTAIM are unclear. Subsequent manuscripts focused on discrediting either the physical basis of EDA,[17] or the predictive power of the QTAIM. Very recently, Poater et al.[18] have extended their arguments to understand the kinked geometry of polycyclic benzenoids.

Central to the discussion and to chemistry itself lies a confusion between pairs of related but different concepts. On one hand we have bonds, which introduce a special relationship among atoms (usually two); and we have binding, related to the energetics of a bound state. On the other hand we use forces among objects, which may be attractive or repulsive, and we speak of stabilizing or destabilizing phenomena, when we turn to the energy scale. An objective use of these concepts should cause no concern to anyone. Unfortunately, this is not what we usually find. No atoms suffer forces in EDA, but systems prepared in well-defined states (independently of their being physically meaningful) suffer energy changes. Who senses the repulsions, or the attractions? And how is the bonding network obtained in EDA? Not from an EDA-consistent framework, but probably from interatomic distances, Mulliken overlap populations, or simple a priori knowledge. Similarly, if equilibrium energies are written as a sum of atomic contributions in QTAIM, to what BP (i.e., bond) do we assign a given energy change? And how do we interpret it, given that at stationary points there are clearly no forces either on the nuclei or the electrons? Even more clearly, at any non-equilibrium geometry (e.g., just coming out of the planar biphenyl and sliding down to the twisted minimum) there will be only (Feynman) forces exerted upon the nuclei, because any (Born–Oppenheimer) wavefunction has an equilibrium electronic system. Upon what objects do the alleged steric repulsions act? The answer from any global procedure such as EDA might be that, overall, the energy increase coming from the antisymmetrization of the fragments' wavefunctions (named Pauli repulsion) accounts for the observed behavior, but rigorously speaking, it should not appeal directly to repulsions between particular atoms.

A quote to the previously cited paper by Haaland, Shorokhov, and Tverdova helps us pinpoint the situation: "Most chemists would probably agree that the defining property of a chemical bond is the existence of a positive bond rupture energy, that is, that the energy of the molecule is lower than the energy of the fragments…". This statement does not allow for metastable bonds, well known and clearly within the scope of Pauling's classical definition[19] of a chemical bond. For instance, the U_2^{2+} cation is unstable with respect to a Coulomb explosion into two U^+ ions,[20] although a barrier greater than 150 kcal mol^{-1} makes it metastable. And the D_{3h} isomer of ozone,[21] which lies about 30 kcal mol^{-1} above the angular minimum, has three equivalent O–O links and liberates energy when one of them is broken to form the usual C_{2v} isomer. Most chemists would probably draw a U–U or three O–O lines in the above cases, in line with Pauling. And on accepting this, the connection between the existence of a particular bond and an overall energetic stabilization becomes complex. Chemical bonds between the host and the cage in He@adamantane are denied by Haaland, Shorokhov, and Tverdova by using their bond-rupture-energy criterion, because the complex is metastable with respect to dissociation, with a large barrier. They would, however, be readily accepted in exothermic compounds, such as B^{3+}@adamantane[8] or Sc_3N@C_{80}.[22,23] The situation would not be so clear had they used Pauling's definition. These simple examples show that in borderline cases there is no general consensus on when and how we should draw a line between two atoms, nor on the relation between these lines and the energy of a molecule.

Here we show that a proper answer to the BP problem, together with a companion energetic image compatible with classical models, exists within the QTAIM. It is based on recognizing in the previous arguments the main drawback of current QTAIM energetic analyses: a lack of interaction energy terms between quantum atoms. The calculation of such terms within a Hartree–Fock scheme was proposed and first computed by Mayer et al.[24,25] Recent algorithmic advances,[26,27] together with the proposal of a fruitful generalized theoretical framework based on the theory of electronic separability of McWeeny,[28] have led to what we have named the interacting quantum atoms (IQA) approach.[29–31] This allows us to write the total energy of a system (E) as a sum of atomic self energies, which contain all the intra-atomic energetic terms, plus a sum of pairwise additive interaction energies between atoms: $E=\Sigma_{\mathrm{A}}E_{\mathrm{self}}^{\mathrm{A}}+\Sigma_{\mathrm{A}>\mathrm{B}}E_{\mathrm{int}}^{\mathrm{AB}}$. The latter are best interpreted as made up of a classical electrostatic component, $V_{\mathrm{cl}}^{\mathrm{AB}}$, and a stabilizing quantum-mechanical correction, $V_{\mathrm{xc}}^{\mathrm{AB}}$, the exchange-correlation potential energy, $E_{\mathrm{int}}^{\mathrm{AB}}=V_{\mathrm{cl}}^{\mathrm{AB}}+V_{\mathrm{xc}}^{\mathrm{AB}}$. The full procedure is orbital invariant.

Our aim is to show that BPs signal privileged, or direct, electron-exchange channels between atoms, and thus contribute to lower their mutual interaction energy. Adequate consideration of the remaining energetic contributions, that is, the classical interaction and the corresponding atomic self energies, demystifies the meaning of BPs, now clear even at

© 2007 Wiley-VCH Verlag GmbH & Co. KGaA, Weinheim

non-equilibrium situations. Moreover, a comparison between IQA and other schemes, such as EDA, is relatively straightforward,[32] contributing to building bridges among conflicting chemical-bonding models. In addition, because in IQA there are sizeable interactions both between bonded (i.e., joined by a BP) and nonbonded atoms, our view should also clarify how a theory with localized BPs, such as QTAIM, is compatible with the non-localized bonding views that are emerging for intermolecular interactions, recently reviewed by Dunitz and Gavezzotti.[33]

To illustrate our arguments, a number of simple systems were selected that exemplify the different concerns around the BP and BCPs concepts described above. Our journey will show how V_{xc} is the quantity related to the appearance of BPs, and how bonds, binding, and forces may be recovered from a single framework.

Theoretical Methods

The IQA approach: As briefly considered in the Introduction, the IQA approach[26,27,29–32] uses a one- and two-basin partitioning of the molecular energy using QTAIM groups [Eq. (1)]:

$$E=\sum_{\mathrm{A}}\int_{\Omega_{\mathrm{A}}}\mathrm{d}\boldsymbol{r}_1\left\{\hat{T}-\sum_{\mathrm{B}}\frac{Z_{\mathrm{B}}}{\boldsymbol{r}_{1\mathrm{B}}}\right\}\rho_1(\boldsymbol{r}_1;\boldsymbol{r}_1')+\frac{1}{2}\sum_{\mathrm{A,B}}\int_{\Omega_{\mathrm{A}}}\mathrm{d}\boldsymbol{r}_1\int_{\Omega_{\mathrm{B}}}\mathrm{d}\boldsymbol{r}_2\frac{\rho_2(\boldsymbol{r}_1,\boldsymbol{r}_2)}{\boldsymbol{r}_{12}}+\sum_{\mathrm{A>B}}\frac{Z_{\mathrm{A}}Z_{\mathrm{B}}}{R_{\mathrm{AB}}} \tag{1}$$

In this expression, Ω_{A} is the basin of nucleus A, and ρ_1, ρ_2 the first- and second-order reduced density matrices, respectively. IQA takes over the above partition, joining energetic terms such that chemically meaningful objects appear, in the light of McWeeny's[28] theory of electronic separability. Thus [Eq. (2)],

$$\begin{aligned}E&=\sum_{\mathrm{A}}(T_{\mathrm{A}}+V_{en}^{\mathrm{AA}}+V_{ee}^{\mathrm{AA}})+\sum_{\mathrm{A>B}}^{\mathrm{A}}(V_{nn}^{\mathrm{AB}}+V_{en}^{\mathrm{AB}}+V_{en}^{\mathrm{BA}}+V_{ee}^{\mathrm{AB}})\\&=\sum_{\mathrm{A}}E_{\mathrm{self}}^{\mathrm{A}}+\sum_{\mathrm{A>B}}E_{\mathrm{int}}^{\mathrm{AB}}\end{aligned} \tag{2}$$

in which we have used an easy-to-decrypt nomenclature in which A,B represents either atom (basin plus nucleus) or groups of atoms (the union of a number of basins and their corresponding nuclei).[29,31,34] Intrabasin contributions define a group's self energy, and all interbasin ones the pairwise-additive interaction energy between pairs of groups. When appropriate group reference energies, $E^{\mathrm{A,ref}}$, are used to define a given binding-energy scale, it is useful to introduce group deformation energies, $E_{\mathrm{def}}^{\mathrm{A}}=E_{\mathrm{self}}^{\mathrm{A}}-E^{\mathrm{A,ref}}$. Binding in IQA results from the competition between group deformation (or promotion, usually positive) and intergroup interaction (overall negative): $E_{\mathrm{bind}}=\Sigma_{\mathrm{A}}E_{\mathrm{def}}^{\mathrm{A}}+\Sigma_{\mathrm{A>B}}E_{\mathrm{int}}^{\mathrm{AB}}$. Interactions are read in the chemical scale by decomposing[27] ρ_2 into coulombic and exchange-correlation contributions, $\rho_2=\rho_2^{\mathrm{C}}+\rho_2^{\mathrm{xc}}$, so that $V_{ee}^{\mathrm{AB}}=V_{\mathrm{C}}^{\mathrm{AB}}+V_{\mathrm{xc}}^{\mathrm{AB}}$. In this way, each intergroup interaction may be divided into a classical, $V_{\mathrm{cl}}^{\mathrm{AB}}=(V_{nn}^{\mathrm{AB}}+V_{en}^{\mathrm{AB}}+V_{en}^{\mathrm{BA}}+V_{\mathrm{C}}^{\mathrm{AB}})$, and an exchange-correlation (nonclassical, quantum) term, $V_{\mathrm{xc}}^{\mathrm{AB}}$. The IQA decomposition provides a means to quantitatively gauge the relative roles of deformation, classical, and nonclassical interactions in different bonding regimes.[29,31] Interesting insights into the origin of the different IQA terms may be found by appealing to electron-population-distribution functions (EDFs) within atomic basins, that is, the probabilities $p(S)$ of a given partition (or real-space resonant structure) S of the n electrons of a molecule into its m basins: $S=(n_1, n_2, \ldots, n_m)$, such that exactly $n_1, \ldots, n_m$ electrons lie within basins $1, \ldots, m$.[35]

Computational details: All wavefunctions were obtained through the GAMESS[36] code by using 6-311G++(d,p) basis sets. Nondynamic correlation effects were incorporated in the smallest systems at the complete active space (CAS) level, using all of the molecular valence electrons and a number of active functions equal to the total number of valence atomic orbitals (full valence CAS). Geometries that fix particular distances or angles were fully optimized for the rest of nuclear degrees of freedom. The IQA analysis was performed by using our PROMOLDEN code. Numerical integrations used atomic β spheres with radii adjusted to 90% of the distance from the nucleus to the nearest basin boundary. Inside the β spheres, restricted angular Lebedev quadratures with 302 points, and 256 points Gauss–Chebychev mapped radial grids were used. l expansions were cut at $l=6$. Outside the β spheres, extended 4000 points Lebedev, 512 mapped radial points trapezoidal quadratures, and l expansions up to $l=10$ were selected. Total energies reconstructed from these IQA decompositions result in accuracies better than 0.5 kcal mol^{-1}. Electron-number distribution functions (EDF) were constructed from the PROMOLDEN basin integrations through our EDF code.

Results and Discussion

BPs signal privileged exchange channels: Any molecular graph built from QTAIM bond paths is necessarily connected, a property emanating from the general features of the electron-density field, and a nucleus may thus be reached from any other by following a series of BPs.

Two interesting limits for understanding the appearance of BPs are clear. At large internuclear distances, as in the case of weak intermolecular interactions, the question reduces to which atoms get directly linked by a BP. In the simplest cases, such as in a He_2 system, the two atoms must share a BP at any separation. The changes of almost all the standard basin (and basin-surface) properties in the approach of two atoms to form diatomic molecules have been fruitfully explored,[37] but the interpretation of BPs based on this faces the problem that many of these quantities (such as the change in the atomic kinetic energy, or the Ehrenfest or Feynman forces) change sign at particular internuclear distances. If the approaching groups have internal structure (e.g., two interacting CO_2 molecules), new degrees of freedom appear, and now we must also understand why some atoms become bonded, and others do not. Interestingly, deep insights into the nature and directionality of intermolecular forces have been obtained by considering BPs in weakly bound systems.[38] Moreover, the promolecular model,[39] which approximates the molecular density by simply adding in vacuo atomic densities and which generally succeeds predicting the topology of ρ in standard molecules, often fails in weak complexes.

At typical interatomic distances, on the other hand, atomic-size coordinates have been used to predict BPs, in line with the work by Cioslowski and Mixon.[9] According to this interpretation, BPs appear whenever two atoms interpenetrate beyond the sum of their van der Waals radii, their BP being nonbonded in the case of two approaching closed shells, for instance. However, it is known that distance (i.e., size) does not complete the picture in this regime, as examples are known of atoms that become better bonded to farther rather than closer neighbors.[40] The particularly clear role of atomic (or ionic) size found in our studies of the topology of ρ in ionic crystals,[10,41] which offers a modern perspective of Pauling's rules for phase preference, clarifies that size dominates whenever the prevailing binding *forces* are not particularly directional. This is the case of the electrostatic binding in alkali halides. As directional quantum-mechanical contributions take over electrostatics, new variables may invalidate the distance rule.

At this point, the plausible role of the exchange-correlation potential energy in determining BPs emerges. We examine this possibility by appealing to three simple processes in which BPs suffer important rearrangements. Two of them are classic examples. The first one (Scheme 1) is the C_{2v} approach of an O(^{1}D) atom to a $^1\Sigma_g^+$ H_2 molecule to form a ground-state water species, in which a BP from the O atom to the H–H BCP changes into the two standard O–H BPs in H_2O.[1] The second process (Scheme 2) is the HCN to CNH isomerization, and the third one (Scheme 3) is an excursion over a portion of the LiF_2^- electronic-energy surface in which a fluoride anion moves around a circle of fixed radius $r = 3.326$ Å centered at the midpoint of a LiF molecule with $d = 1.653$ Å passing from a FLiF to a LiFF configuration. All of these processes were computed at the full-valence CAS level, with evolution coordinates as follows: the d distance in **1**; the $\sphericalangle$H*cm*C θ angle (*cm* standing for the center of mass of the CN subsystem) in **2**; and the α coordinate in **3**. In this last system, the CAS optimization fails to converge if $\alpha \lesssim 40°$, but this is not a severe problem for our purposes.

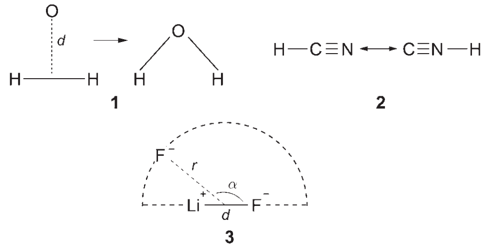

Scheme 1. Geometrical parameters in processes **1**–**3**.

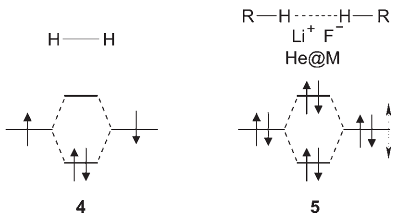

Scheme 2. Conventional view of two-orbital, two-electron attractions vs. two-orbital, four-electron repulsions.

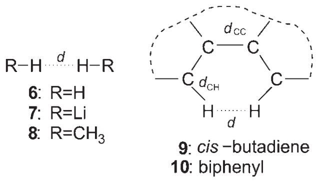

Scheme 3. Systems with H–H interactions.

From the energetic point of view, process **1** proceeds from the large d limit through a small barrier of about 2 kcal mol^{-1} at $d \approx 2.0$ Å, when the HOH angle is 21.6° and the H–H distance has increased by 0.005 Å towards the deep H_2O well at $d = 0.602$ Å, 147 kcal mol^{-1} below the O(^{1}D) + H_2($^1\Sigma_g^+$) limit. For our purpose, this exemplifies the competition between the weak O–(H_2) plus strong covalent H–H interactions at large d, and the two heteropolar O–H links in water. Similarly, the HCN to CNH isomerization, which proceeds through a 53 kcal mol^{-1} barrier at $\theta = 77.8°$ towards a CNH product 15.9 kcal mol^{-1} above the HCN moiety, serves as a more subtle example of competition between the H–C and H–N links. Finally, process **3** displays a continuous energy increase of about 100 kcal mol^{-1} as α goes from 180 to 0°, dominated by electrostatic interactions, but with a BP change from Li–F to F–F.

The topological changes suffered in these ABC rearrangements are well understood.[1] System **1** passes through an ephemeral ring structure, with both O–H and H–H BPs, formed at $d \approx 1.391$ Å and destroyed at $d \approx 1.389$ Å to collapse on the water molecular graph. Processes **2** and **3** result in a conflict catastrophe at $\theta \approx 76°$, and $\alpha \approx 110.5°$, respectively. It is important to notice that the existence of barriers or transition states is not directly related to topological changes. In **1**, the catastrophe occurs about 30 kcal mol^{-1} below the transition state, in **2** it lies close to the barrier, but at definitely different θ values, and in **3** there is topological change without energetic stationary point. When and why does an atom prefer one BP over the other?

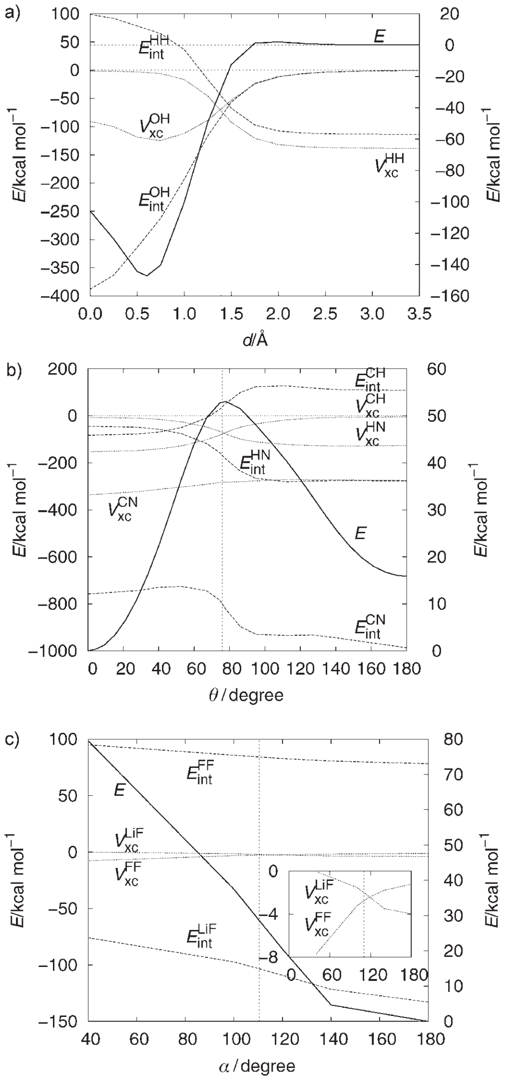

Figure 1. Evolution of relevant IQA interaction components in the **1** (top), **2** (center), and **3** (bottom) processes along their corresponding evolution coordinates. Total molecular energies are also plotted as thick full lines that should be read on the right energetic scale. The V_{xc} crossing in system **3** is enlarged as an inset (bottom). Topological changes are indicated by vertical dotted lines.

The image released by examining the IQA interactions is revealing, as shown in Figure 1. In **1**, at large d values an isolated oxygen atom starts interacting with a previously existing H_2 molecule. The only important interaction in this regime, which persists until the top of the small energetic barrier, is the H−H one. This, as an archetypal nonpolar covalent link,[29,42] is in turn dominated by the V_{xc}^{HH} term, with a small destabilizing classical component. As d decreases E_{int}^{HH} increases, first as an almost pure exchange (covalent) phenomenon, but soon after the barrier is surmounted, a rather sudden charge separation introduces large electrostatic components in the interactions. The OH link gains importance, becoming dominated by the deeply stabilizing V_{cl} term, and V_{xc}^{HH} becomes negligible, with a destabilizing E_{int}^{HH} coming from the classical repulsion between the equally charged hydrogen atoms. The spin couplings among the electrons lying within the hydrogen basins draw a simple chemical process: As the oxygen atom approaches, the initially spin-paired electrons of the H_2 molecule lose their spin coherence, which is regained by electrons in the oxygen basin. For instance, the probability $\rho(n_{H1}=1, n_O=8, n_{H2}=1)$ that each of the hydrogen atoms bears one electron is 0.579 at $d=3.0$ Å, only slightly below that in a free H_2 molecule, 0.583. 100 % of these cases correspond to a ↑↓ (or ↓↑) coupling in both hydrogens. In contrast, at $d=0.5$ Å $p(1,8,1)$ has decreased to 0.112, and only 50.02 % of these cases are now spin-paired ones, showing that the hydrogen electrons have almost independent spin. Spin pairing, one of the most clear-cut features in traditional bond theory, supports the HH link being substituted by two OH ones, independently of any concomitant charge transfer among the basins and, thus, of its associated electrostatic component.

As shown in Figure 1, a given hydrogen atom chooses to be topologically linked through a BP with the atom that provides the larger exchange-correlation stabilizing interaction (i.e., the largest energetic contribution due to spin pairing). The $V_{xc}^{HH}=V_{xc}^{OH}$ event occurs at $d=1.379$ Å, very near the topological change. Interestingly, $p(1,8,1)=0.778$ at $d=1.39$ Å, very close to the 3/4 value that one might expect from a 50 % broken H−H bond. The correspondence between topological change and V_{xc}, which was initially sought, and not found with the position of transition states in energy landscapes, is a strong indication of the role of BPs as preferential exchange channels.

The HCN isomerization[43] provides a more subtle example of BP competition, with a total molecular-energy scale one order of magnitude smaller than that in process **1**, even though the IQA results are qualitatively identical. As noticed previously,[31] the main reason underlying the greater stability of the HCN isomer is the more covalent character of the HC versus the HN interaction. Notice how in the CNH energetic region the CH interaction is basically electrostatic, and the HN and CN ones display both large electrostatic and exchange-correlation components. At the HCN end the situation has changed dramatically, and CN is now the only pair with a relevant ionic-interaction term. Again, V_{xc}^{HC} and V_{xc}^{HN} cross at almost exactly the conflict catastrophe point, which this time is also very near the top of the overall energetic barrier. The total HC and HN interaction energies do also cross, but at much smaller angles.

Finally, process **3** was chosen to demonstrate the secondary role of classical electrostatics in determining BPs. Interestingly, the absolute values of the topological charges of the three atoms are greater than 0.93 e during all the process, so very ionic interactions indeed determine the total molecular energy. At any α angle, E_{int}^{FF} is positive and large, as expected, so the interaction between the two anions destabilizes the system. The contrary holds for E_{int}^{LiF}. Interestingly, the exchange-correlation V_{xc} components are the only energetic terms of comparable magnitude (see the inset in

Figure 1, a few kcals mol^{-1}), and become equal at about $\alpha \approx 120°$, near the, but definitely at a larger α angle than, the conflict point. The fact that the F^{-}–F^{-} BP appears when there is a substantial increase in V_{xc}^{FF} relative to V_{xc}^{LiF} should help to settle the controversy around the role of anion–anion BPs. They signal, as in other less-disputed cases, predominantly stabilizing exchange interactions, whose presence is almost compulsory in condensed phases, independent of the overall repulsion due to electrostatic effects. Similar comments apply to the nature of the stabilizing interactions found in the halogen–halogen synthons used in crystal engineering.[44]

In summary, the primary factor determining the appearance of BPs is exchange (or exchange-correlation), which in more chemical terms may be read as the energetic counterpart of spin pairing. In the absence of long-range delocalization, this contribution is strongly anisotropic, and decays exponentially with the intercenter distance.[31] In its strong regime, that is, $V_{xc} \approx$ tens of kcal mol^{-1}, it gives rise to the traditionally directional covalent forces, and the rules of valence apply to BPs. In contrast, if nondirectional electrostatic terms dominate the interactions, a case common in ionic crystals with V_{xc} values closer to 1 kcal mol^{-1}, distance becomes important, size coordinates gain relevance, and Pauling's rules are uncovered.[41] In the case of weak, non-electrostatic interactions, a mixture of distance and residual-directionality criteria will determine which BPs exist.

Overall closed-shell destabilizations are compatible with local stabilizing interactions: We are now in a position to understand the meaning of other controversial BPs, as in our previously commented endohedral or hydrogen–hydrogen bonding cases. In one way or another, they all may be viewed as the standard "repulsive" two-orbital, four-electron interactions in molecular orbital (MO) theory, opposed to the bonding two-orbital, two-electron case of H_2 (Scheme 2). Notice that by sliding one of the interacting orbitals in **5** we may also include the Li^{+}–F^{-} case in the first class, stabilized by electrostatics. We will focus here on the H–H problem, which will provide insights of quite general validity.

A blind translation of the concepts developed so far would lead us to predict that, as soon as the stabilizing V_{xc} term between the "sterically" crowded atoms would become intense enough, that is, at a sufficiently short distance that would depend on the nature, number of electrons, and size of their nearest neighbors, a BP would develop. Furthermore, for typical R-C-H···H-C-R′ interactions with negligible net charges on the hydrogen atoms, we would predict a window of H–H distances with total stabilizing E_{int}^{HH}. This is exactly the behavior found. To exemplify this, we will summarize some results obtained in the systems of Scheme 3.

These results include the head-to-tail approach of two identical molecules: H_2 in **6**, LiH in **7**, and methane keeping a D_{3d} symmetry in **8**, all of them with a dissociating minimum configuration (see, however, the discussion on **7** below). They also include the intramolecular H–H interactions between the closest 1,4 hydrogens in planar *cis*-butadiene, **9**, and the 2,8 *ortho* hydrogens in the planar and twisted geometries of biphenyl, **10**. All degrees of freedom except the relevant H–H distances d in **6**–**9** were optimized. Because the computation of interactions in biphenyl is a difficult computational task, we have restricted our wavefunctions to the Hartree–Fock level and, for consistency, the same was done in **6**, **8**, and **9**. Systems **6** and **7** were also computed at the CAS level previously described.

From the structural point of view, it is experimentally known[45] that biphenyl has a twisted structure with a dihedral angle between the phenyl planes $\phi = 44.4°$, and a planar transition state 1.4 kcal mol^{-1} above the twisted structure (another perpendicular one will not be considered here). Any reasonable wavefunction (including a minimal basis HF//STO-3G calculation) predicts a twisted minimum that increases in energy towards the planar structure. In our case $\phi = 44.6°$ and $\Delta E = 3.3$ kcal mol^{-1}, showing that the HF model contains all the necessary elements to understand the problem. Changing from the twisted to the planar structures induces a large decrease in the d distance between the *ortho* hydrogens, from 2.488 to 1.963 Å, coupled to a slight increase in the interphenyl d_{CC} distance of 0.01 Å and a small decrease of 0.003 Å in the *ortho* d_{CH} distance. These have been traditionally interpreted as signs of "steric crowding". Similar results hold as d is constrained to decrease from its optimum value in *cis*-butadiene, $d = 2.34$ Å. For instance, at $d = 1.52$ Å, $\Delta d_{CC} = 0.007$ and $\Delta d_{CH} = 0.009$ Å, respectively. We have found that the behavior of d_{CH} (or its equivalent d_{RH} in **6**, **7**, and **8**) depends on the type of constraint imposed on the H–H distance. If d_{RR} is constrained, then the hydrogen atoms are forced into local Feynman-force equilibrium, and d decreases. This is also found in planar biphenyl, in which the phenyl–phenyl link acts as an external d_{RR} constrain. If, on the contrary, it is d itself that is artificially fixed, then the R groups are forced to local equilibrium, and d_{RH} increases, as found in **9**. Again, this behavior has usually been understood in terms of "closed-shell repulsions". Overall destabilization is not necessarily coupled to destabilizing local interactions.

From the topological front, systems **6**–**8** do not display molecular graph changes in wide d regions, and BCPs appear at the midpoint of the HH segment at any d value. As is well known, the same BPs exist in H_2 and in He_2. In contrast, **9** and **10** show topological changes, and on going from the twisted to the planar biphenyl a BP appears between the *ortho* hydrogens. Similarly, a H–H path is formed in **9** at $d \approx 2.25$ Å. We should notice the proximity of the planar configuration of *cis*-butadiene to the formation of a H–H bond path.

We have plotted in Figure 2 the H–H interaction energy, as well as its exchange component (no correlation at the HF level) in systems **6**, and **7**–**10**. Several important facts should be noted. First, the "closed-shell" E_{int}^{HH} curves have a characteristic Morse-type shape with a developed 20 kcal mol^{-1} minimum at about $d = 0.9$ Å. Moreover, the curves are rather universal, more so at distances beyond the minimum,

© 2007 Wiley-VCH Verlag GmbH & Co. KGaA, Weinheim

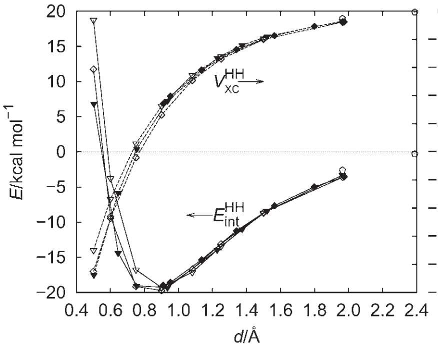

Figure 2. Hartree–Fock E_{int}^{HH} and V_{xc}^{HH} energies as a function of d in systems: **6**, by ◇ and ◆ if d or d_{RR} are constrained, respectively; **8**, by ▽; and **9**, by ▼. The interaction energies in planar (**10**, $d=1.96$ Å) and twisted biphenyl ($d=2.39$ Å) are also plotted with open pentagons.

and only reveal the particular nature of the system examined at small d values. Similar comments apply to V_{xc}^{HH}. This reasonable universality, or transferability of the interaction, is a strong point favouring the existence of H–H bonding. The interaction in planar biphenyl nicely fits this image, with $E_{int}^{HH}=-2.6$ and $V_{xc}^{HH}=-3.75$ kcal mol^{-1}. Its twisted ground state has a $d=2.39$ Å. Consistently, $E_{int}^{HH}=-0.3$ and $V_{xc}^{HC}=-0.98$ kcal mol^{-1}. Notice also how the interaction tends to its exchange component at large distance, V_{cl}^{HH} decays more quickly than V_{xc}^{HH}, and that the latter is more transferable than the total interaction. It is easy to prove that when two equivalent-by-symmetry atoms interact, their V_{cl} interaction is necessarily positive.[31] This is the origin of the destabilizing wall in Figure 2 at short H–H distances, when the nuclear–nuclear and electron–electron repulsions dominate over the electron–nucleus attraction. In summary, Figure 2 shows how exchange between the electrons in both hydrogen basins gives rise to an interaction-energy image that cannot be easily distinguished from that found in a (weak) covalent link.

Having ascertained the stabilizing nature of the H–H interaction in the systems presented above, and its exchange origin, an important point remains to be understood, namely, the nature of the overall energetic destabilization of the systems as d decreases. One of the advantages of IQA and other real-space analyses is its locality. Thus, if the phenomena under study have a short-range root, it will emerge naturally. This is our case, and we found that ΔE is almost completely determined by a small subset of atoms, particularly involved in the process, which we will call G, such that $\Delta E \approx \Sigma_{A \in G} \Delta E_{self}^{A} + \Sigma A > B, \in G \Delta E_{int}^{AB}$. For instance, the approach of the two methane molecules in **8** is energetically reconstructed within a couple of kcal mol^{-1} by considering the C–H···H–C subgroup. In the regime in which the "steric" H–H interaction is stabilizing, $\Delta E > 0$ is clearly possible by a larger energetic counterbalance, due to a change in either the other interactions, or the self energies of the atoms within ς. Without loss of generality, system **6** (H3–H1···H2–H4) is perfectly suited to analyze these effects in detail. We will use Hartree–Fock functions to allow for a direct comparison between IQA and EDA results, with constrained d_{H3H4} optimizations.

Two $d=d_{H3H4}$ distances, 3.000 and 2.187 Å, with corresponding H1H2 separations equal to 1.564 and 0.911 Å were selected (systems **6a** and **6b**, respectively). For comparison, the free H_2 equilibrium is obtained at 0.746 Å. All relevant IQA results are gathered in Table 1, and total ΔE values with respect to $d \rightarrow \infty$ are 5.1 and 53.7 kcal mol^{-1}, respectively. As shown in Table 1, the increase in self energy (measured with respect to self energies at the equilibrium geometry of H_2) are very localized at the interacting side of each molecule (H1, H2). In fact, we found that the small negative deformations of the other end atoms are quite general in closed-shell interactions. Notice also how the intramolecular interactions (−137.7 kcal mol^{-1} in free H_2) decrease in magnitude as the two molecules approach. In a qualitative sense, the pre-existing interaction of H1 with H3 becomes shared with H2 as d decreases.

Table 1. Some IQA energetic quantities [kcal mol^{-1}] in the Hartree–Fock H3–H1···H2–H4 system. The deformation energies (ΔE_{self}) are obtained with respect to the optimum free H_2 molecule, with $E_{int}^{H1H2}=-137.7$ and $E_{xc}^{H1H2}=-163.6$ kcal mol^{-1}, respectively. All energies in kcal mol^{-1}.

	6a	**6b**
d [Å]	1.564	0.911
ΔE_{self}^{H3}	−0.5	−0.8
ΔE_{self}^{H1}	6.3	28.3
ΔE_{int}^{H1H2}	−7.7	−19.0
ΔE_{int}^{H1H3}	−135.2	−122.7
ΔE_{int}^{H1H4}	−1.6	−3.3
ΔE_{int}^{H3H4}	−0.7	−5.8
V_{xc}^{H1H2}	−8.7	−32.8
V_{xc}^{H1H3}	−164.3	−162.2
V_{xc}^{H1H4}	−1.9	−5.2
V_{xc}^{H3H4}	−0.9	−6.5
E_{def}^{H1H3}	8.3	42.5
$E_{int}^{H1H3,H2H4}$	−11.6	−31.4
$V_{xc}^{H1H3,H2H4}$	−13.4	−44.5

It is fruitful to construct the self energy of each H_2 molecule in the dimer, $E_{self}^{H_2}=E_{self}^{H1}+E_{self}^{H3}+E_{int}^{H1H3}$. In this way, the total ΔE is twice the deformation energy of each individual monomer, E_{def}^{H1H3}, plus the interaction energy between them, $E_{int}^{H1H3,H2H4}$. The latter may be clearly decomposed into exchange(-correlation) and classical components. Deformation of the monomers, mainly driven by deformation of the directly interacting hydrogen atoms, but also by the decrease in strength of each intramolecular H–H bond, is thus the origin of the observed destabilization.

Even more insight may be gained if we add into a single quantity all the deformations and intermolecular exchange interactions. As we have previously shown,[32] this is the IQA equivalent to the Pauli repulsion or exchange–repulsion (XR) term in the EDA decomposition, and we will call it XR(IQA). In the present case, $\text{XR(IQA)}=2E_{def}^{H1H3}+V_{xc}^{H1H3,H2H4}$.

In EDA, the interaction between two prepared monomers is written as $\Delta E_{int}=\Delta V_{elstat}+\Delta E_{Pauli}+\Delta E_{oi}$. The first term is the classical electrostatic interaction between the interpenetrating fragments. This ΔV_{elstat} is a generally stabilizing quantity that has received much interest in recent years.[46,47] When densities do not interpenetrate, as in topological approaches, its equivalent is usually much smaller, and destabilizing[30,31] if charge transfer between the fragments is not important. The energy distance between the unmodified electrostatically interacting fragments and the wavefunction obtained by antisymmetrizing (and renormalizing) the (geometrically prepared) wavefunctions of the isolated monomers, Ψ^0, is the XR or Pauli repulsion term, ΔE_{Pauli}. To this, a self consistency or orbital-interaction stabilization, ΔE_{oi}, is added that leads to the final ΔE_{int}. An interesting feature of our present procedure is that one may also perform an IQA analysis from the Ψ^0 wavefunction, which allows for an almost direct comparison with EDA.[32]

EDA leads to $\Delta V_{\text{elstat}}=-1.3$ and -5.2 kcal mol^{-1}, and to $\Delta E_{\text{Pauli}}=8.3$ and 70.5 kcal mol^{-1} for systems **6a** and **6b**, respectively. Thus, the "Pauli repulsion" term is invoked by Poater, Solà, and Bickelhaupt[13] as clear support of the "steric repulsion" image of this kind of H–H interaction. From Table 1, XR(IQA) is 3.2 and 40.5 kcal mol^{-1} in **6a** and **6b**, respectively. Although these values are smaller than the EDA ones, as indeed they should be, they are positive and evolve in similar ways. In fact, both the deformation and exchange components of XR(IQA) are almost saturated if computed from the Ψ^0 antisymmetrized function. This is the same behavior already found in hydrogen-bonded dimers,[32] and shows how enlarging the size of the Hilbert space upon interaction is the main reason for both the deformation and exchange energies of the fragments.

Now a unifying frame emerges. By using ΔE_{Pauli}, a nonlocal quantity of the fragments upon interaction, the fact that it actually brings together *local* destabilizing (deformation) and stabilizing (exchange) contributions is missed. Thus, although deformation prevails over exchange, and $\Delta E>0$, there are well-defined exchange channels between the H1 and H3 atoms with their related BPs.

Underlying the exchange-correlation term between the "sterically crowded" hydrogen atoms of this work, spin pairing appears again. For instance, in system **6b**, the total probability that one and only one electron occupies each of the H1 and H3 basins is 0.413, well below the 0.5 isolated-molecule HF value. 99.9 % these configurations correspond to spin-paired (↑↓ or ↓↑) couplings, so there is still a strong H1H3 link. There is also an overall 0.24 probability of finding one electron in each of the H1 and H2 basins, 62 % of them spin paired. This implies a 12 % excess over the independent-molecules value, and a partial bond being formed. Similarly, the large positive deformations are equally understood by noticing that delocalization between the molecules introduces a probability of 8.4 % that the H1H3 molecule bears three electrons. As we have recently shown,[48,49] these overcrowded, confined resonant structures increase the atomic self energies (E_{self}) significantly, particularly when no new spin pairings occur. In agreement with conventional wisdom, simple closed-shell interactions such as those in R–H···H–R systems lead to "repulsion" due to a competition between stabilizing RH and HH pairings on one hand, and destabilizing deformations due to delocalization, and which may be interpreted as due to Pauli exclusion, on the other.

We should stress that our view emphasizes the similar nature of the physical processes that lead to the stabilizing $V_{\text{xc}}^{\text{HH}}$ term in both the R–H···H–R closed-shell systems and in the paradigmatic open-shell H_2 case: spin pairing. This is, by no way, a statement about similar chemical bonds for closed and open shells. As shown, self energies behave very differently in both cases. They increase very quickly in the former, thus justifying the overall destabilization, whereas $\Delta E_{\text{self}}^{\text{H}}$ is kept at a 8 kcal mol^{-1} level in H_2 at R_e.[29] Local interactions are thus similar in closed- and open-shell cases, but deformation energies are not. The overall *chemical bond* is thus completely different in the two cases.

Figure 2 shows that the H–H exchange grows as d decreases. Might then the "repulsion" come to an end at a given small d value? This illuminating possibility was explored in system **7**, which has the interesting property that a H_2 bond is stronger than two LiH ones. At the valence CAS level, the $2\,\text{LiH}\rightleftharpoons H_2+2\,\text{Li}$ reaction is thus exothermic by 6.5 kcal mol^{-1}. Some interesting effects should thus be expected on decreasing d in a head-to-tail manner.

As shown in Figure 3, the transition occurs. As d decreases, the LiH distance in each of the approaching molecules slightly increases, and a normal closed-shell destabilization occurs. At $d\approx 1.21$ Å a relatively sudden collapse forces the two Li atoms apart, these remain loosely bound at about 5 Å from their nearest hydrogen atoms if d is further decreased, and a H_2 molecule forms. Severe density reorganizations transform the almost Li^+ basins in the 2 LiH region to neutral lithiums beyond the top of the barrier. There is no topological change, because Li–H and H–H BPs exist at all d values, but as we might likely have expected from our previous arguments, the competition between the H^- singlet pairing present in each LiH molecule at large d, and the covalent H–H one in the $2\,\text{Li}+H_2$ at short d is clear. At about

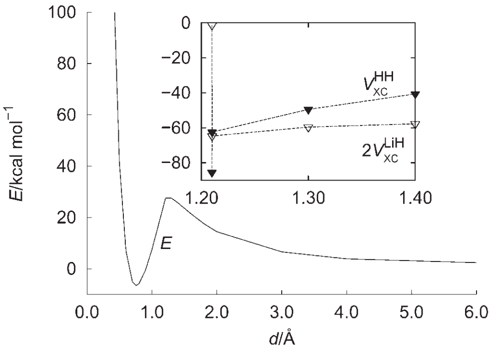

Figure 3. Total energy and relevant exchange-correlation components for the head-to-tail approach of two LiH molecules at the CAS level. Only V_{xc} is shown in the inset within a small d window near the top of the energy barrier.

the collapse geometry, $2V_{xc}^{LiH}$ becomes almost degenerate with V_{xc}^{HH}. Beyond this point, it is clearly preferable to pair the electrons in the HH region and force the Li atoms apart. We may follow the HH spin pairing as in previous cases. Just before the collapse, for instance, there is a probability of 0.038 to find just one electron in each of the two hydrogen basins (leaving two neutral Li atoms). However, these two electrons are already spin paired in 70 % of cases. Notice how the exchange between the hydrogen atoms is much more intense than between the H^- and Li^+ ions in the LiH molecules.

Conclusion

We have presented compelling evidence showing how the bond paths of the quantum theory of atoms-in-molecules signal the existence of preferred or privileged exchange channels in molecules (strictly speaking, exchange-correlation channels). These channels are nothing but real-space carriers of quantum-mechanical exchange.

This goal was achieved by substituting the standard one-basin energy decomposition of the theory by the IQA framework, based on an exact one- and two-basin decomposition of the molecular energy. The one-basin terms provide the atomic self energies, E_{self}, and the two-basin ones their interaction energies, E_{int}. Because the interaction between two atoms is treated explicitly in IQA, the approach provides fruitful insights into chemical-bonding problems. Interaction energies are pairwise additive, and may be decomposed into a classical term, V_{cl}, that measures the total electrostatic interaction between the atomic densities, and a quantum-mechanical correction coming from the exchange-correlation second-order density, V_{xc}. The latter is a stabilizing contribution that may be either enhanced, or counterbalanced by the classical term. Overall energetic binding results when attractive E_{int} overcome the general E_{self} destabilization that accompanies interaction.

By examining a number of archetypal simple systems, we have shown that a bond path is found between two atoms when: 1) there is no other competing atom in its vicinity, so there must be a direct exchange route between them; 2) its V_{xc} term with that atom is the largest among several possibilities. Thus, BPs indicate particularly important exchange-correlation terms, necessarily lowering the energy of the system. This interpretation agrees with QTAIM orthodoxy, both in its virial[6] and Ehrenfest[8] versions.

However, a note of caution should be made. The existence or absence of a BP is related to the competition of different exchange channels, and not to the absolute value of exchange-correlation energies. For instance, when no competition is present, as in the He–He case, a BP will appear independently of the value of V_{xc}^{HeHe}. Moreover, there might be systems in which, despite a large V_{xc}, a BP is not formed between two atoms because privileged channels of exchange interaction, other than the bond path, come into play, for example, those channels associated to lone pairs.

A stabilizing local interaction does not imply, however, that the total energy of a system falls. This is the basis to understand why closed-shell interactions, such as those present in the recently proposed hydrogen–hydrogen bonds,[12] lead to an overall energy increase despite non-negligible negative HH exchange-correlation energies. As shown with several examples, it is the self-energy change of the hydrogens and their nearest neighbors that accounts for the positive sign of ΔE. The inability of non-local energy analyses such as EDA to isolate local contributions to the energy allows us to understand why these methods only "sense" the final repulsion. IQA dissects its origin. Many other criticized BPs, such as those between anions in condensed phases, or between encapsulated molecules and their cages in endohedral complexes, also have a clear meaning with our arguments.

The image proposed here establishes a connection between bond lines (bonding) and energetics (binding): the former are linked to the exchange-correlation component of the interaction energy between a pair of atoms. A translation of this link into the traditional (binding-like) image of chemical bonds is not straightforward, for it must also include the electrostatic part of the interaction and the atomic self energies, which do not directly determine the existence of bond lines. Bond paths sense stabilizing exchange-correlation channels, but not global energy changes. Thus, they are compatible with global energy increases.

We have also shown that, from a chemical point of view, the HH closed-shell interaction energies do not differ essentially from those in other accepted bonds. Their origin lies in a partial spin pairing of the associated electrons that increases as the magnitude of V_{xc} increases. In extreme cases, such as in our LiH dimer example, one hydrogen may even prefer binding to the other and expel its Li companion if the H–H distance becomes small enough. This does not at all mean that the closed-shell HH global *bonding* is similar to that found in open-shell cases: self energies behave in completely diverging ways, rising quickly in the former case as a result of Pauli's principle.

Our arguments are extendable to other closed-shell contacts, and might shed light on basic aspects of theories of molecular recognition in organic crystals and crystal engineering, or in the construction of more reliable intermolecular force fields.

In summary, bond paths retain a clear meaning for chemistry if the view proposed in this work is embraced. Our interpretation is valid both for equilibrium and non-equilibrium geometries, and compatible with other energy analyses. Strictly speaking, bond paths and binding energies (and so chemical bonds in the too-strict, purely thermodynamic point of view) are not directly related. Recognizing that two-atom bond energies cannot be rigorously defined in polyatomics, but that atomic-like self energies and pairwise additive interactions do persist for atoms within molecules, will be an important step in superseding the molecule-as-a-sum-of-bonds image.

© 2007 Wiley-VCH Verlag GmbH & Co. KGaA, Weinheim

Acknowledgement

Financial support from the Spanish MEC, Project No. CTQ2006-02976 and the ERDF of the European Union, is acknowledged.

---

[1] R. F. W. Bader, *Atoms in Molecules*, Oxford University Press, Oxford, **1990**.

[2] P. Cassam-Chenai, D. Jayatilaka, *Theor. Chem. Acc.* **2001**, *105*, 213.

[3] R. F. W. Bader, *Theor. Chem. Acc.* **2001**, *105*, 276.

[4] R. F. W. Bader, *Theor. Chem. Acc.* **2002**, *107*, 381.

[5] L. J. Farrugia, C. Evans, M. Tegel, *J. Phys. Chem. A* **2006**, *110*, 7952.

[6] T. A. Keith, R. F. W. Bader, Y. Aray, *Int. J. Quantum Chem.* **1996**, *57*, 183.

[7] R. F. W. Bader, *J. Phys. Chem. A* **1998**, *102*, 7314.

[8] R. F. W. Bader, D.-C. Fang, *J. Chem. Theory Comput.* **2005**, *1*, 403.

[9] J. Cioslowski, S. T. Mixon, *J. Am. Chem. Soc.* **1992**, *114*, 4382.

[10] A. Martín Pendás, A. Costales, V. Luaña, *J. Phys. Chem. B* **1998**, *102*, 6937.

[11] A. Haaland, D. J. Shorokhov, N. V. Tverdova, *Chem. Eur. J.* **2004**, *10*, 4416.

[12] F. Matta, J. Hernández-Trujillo, T.-H. Tang, R. F. W. Bader, *Chem. Eur. J.* **2003**, *9*, 1940.

[13] J. Poater, M. Solà, F. M. Bickelhaupt, *Chem. Eur. J.* **2006**, *12*, 2889.

[14] J. Poater, M. Solà, F. M. Bickelhaupt, *Chem. Eur. J.* **2006**, *12*, 2902.

[15] T. Ziegler, A. Rauk, *Inorg. Chem.* **1979**, *18*, 1558.

[16] T. Ziegler, A. Rauk, *Inorg. Chem.* **1979**, *18*, 1755.

[17] R. F. W. Bader, *Chem. Eur. J.* **2006**, *12*, 2902.

[18] J. Poater, R. Visser, M. Solà, F. M. Bickelhaupt, *J. Org. Chem.* **2007**, *72*, 1134.

[19] *".. there is a chemical bond between two atoms or groups of atoms in the case that the forces between them are such as to lead to an aggregate with sufficient stability to make it convenient for the chemist to consider it as an independent molecular species." L. Pauling, The Nature of the Chemical Bond*, 3rd ed., Cornell University Press, Ithaca, N.Y., **1960**.

[20] L. Gagliardi, P. Pyykkö, B. Roos, *Phys. Chem. Chem. Phys.* **2005**, *7*, 2415.

[21] P. G. Burton, M. D. Harvey, *Nature* **1977**, *266*, 826.

[22] J. M. Campanera, C. Bo, J. M. Poblet, *Angew. Chem.* **2005**, *117*, 7396; *Angew. Chem. Int. Ed.* **2005**, *44*, 7230.

[23] J. M. Campanera, C. Bo, J. M. Poblet, *J. Org. Chem.* **2006**, *71*, 46.

[24] I. Mayer, A. Hamza, *Theor. Chem. Acc.* **2001**, *105*, 360.

[25] P. Salvador, M. Duran, I. Mayer, *J. Chem. Phys.* **2001**, *115*, 1153.

[26] A. Martín Pendás, M. A. Blanco, E. Francisco, *J. Chem. Phys.* **2004**, *120*, 4581.

[27] A. Martín Pendás, E. Francisco, M. A. Blanco, *J. Comput. Chem.* **2005**, *26*, 344.

[28] R. McWeeny, *Methods of Molecular Quantum Mechanics,* 2nd ed., Academic Press, London, **1992**.

[29] M. A. Blanco, A. Martín Pendás, E. Francisco, *J. Chem. Theory Comput.* **2005**, *1*, 1096.

[30] E. Francisco, A. Martín Pendás, M. A. Blanco, *J. Chem. Theory Comput.* **2006**, *2*, 90.

[31] A. Martín Pendás, M. A. Blanco, E. Francisco, *J. Comput. Chem.* **2007**, *28*, 161.

[32] A. Martín Pendás, M. A. Blanco, E. Francisco, *J. Chem. Phys.* **2006**, *125*, 184112.

[33] J. D. Dunitz, A. Gavezzotti, *Angew. Chem.* **2005**, *117*, 1796; *Angew. Chem. Int. Ed.* **2005**, *44*, 1766.

[34] A. Martín Pendás, E. Francisco, M. A. Blanco, *Faraday Discuss.* **2007**, *135*, 423.

[35] A. Martín Pendás, E. Francisco, M. A. Blanco, *J. Phys. Chem. A* **2007**, *1084*, 111.

[36] M. W. Schmidt, K. K. Baldridge, J. A. Boatz, S. T. Elbert, M. S. Gordon, J. H. Jensen, S. Koseki, N. Matsunaga, K. A. Nguyen, S. J. Su, T. L. Windus, M. Dupuis, J. A. Montgomery, *J. Comput. Chem.* **1993**, *14*, 1347.

[37] J. Hernández-Trujillo, R. F. W. Bader, *J. Phys. Chem. A* **2000**, *104*, 1779.

[38] R. G. A. Bone, R. F. W. Bader, *J. Phys. Chem.* **1996**, *100*, 10892.

[39] M. A. Spackman, E. N. Maslen, *J. Phys. Chem.* **1986**, *90*, 2020.

[40] V. Luaña, A. Martín Pendás, A. Costales, G. A. Carriedo, F. J. García-Alonso, *J. Phys. Chem. A* **2001**, *105*, 5280.

[41] M. A. Blanco, A. Costales, A. Martín Pendás, V. Luaña, *Phys. Rev. B* **2000**, *62*, 12028.

[42] A. Martín Pendás, E. Francisco, M. A. Blanco, *J. Phys. Chem. A* **2006**, *110*, 12864.

[43] Y. Tal, R. F. W. Bader, T. T. Nguyen-Dang, M. Ojha, *J. Chem. Phys.* **1981**, *74*, 5162.

[44] F. F. Awwadi, R. D. Willett, K. A. Peterson, B. Twanley, *Chem. Eur. J.* **2006**, *12*, 8952.

[45] A. Almenningen, O. Bastiansen, L. Fernholt, B. N. Cyvin, S. J. Cyvin, S. Samdal, *J. Mol. Struct.* **1985**, *128*, 59.

[46] F. M. Bickelhaupt, E. J. Baerends, *Rev. Comput. Chem.* **2000**, *15*, 1.

[47] G. Frenking, F. Wichmann, N. Frölich, C. Loschen, M. Lein, J. Frunzke, V. M. Rayón, *Coord. Chem. Rev.* **2003**, *238–239*, 55.

[48] A. Martín Pendás, E. Francisco, M. A. Blanco, *J. Phys. Chem. A* **2007**, *111*, 1084.

[49] A. Martín Pendás, E. Francisco, M. A. Blanco, *Chem. Phys. Lett.* **2007**, *437*, 287.

Received: March 12, 2007
Revised: June 4, 2007
Published online: August 2, 2007